Elasto-plastic modeling of wood bolted connections

N. Kharouf [a], G. McClure [a,*], I. Smith [b]

[a] *Department of Civil Engineering and Applied Mechanics, McGill University, 817 Sherbrooke Street, West Montreal, QC H3A2K6, Canada*
[b] *Faculty of Forestry and Environmental Management, University of New Brunswick, Fredericton, NB E3B6C2, Canada*

Abstract

A plasticity based constitutive compressive material model is proposed to model wood as elasto-plastic orthotropic according to the Hill yield criterion in regions of bi-axial compression. Linear elastic orthotropic material response is applied otherwise with maximum stresses taken as failure criteria. The model is implemented in the finite element code to carry out the analysis of bolted connections using ADINA software. Reasonable agreement is found between numerical simulations and experimental measurements of local and global deformation of one-bolt connection. The predicted failure modes are consistent with experimental observations.
© 2003 Elsevier Science Ltd. All rights reserved.

Keywords: Elasto-plasticity; Orthotropic; Wood; Bolted connections

1. Introduction

The mechanical behaviour of wood connections with relatively low member thickness to bolt-diameter-ratio is very complex and is influenced by a number of geometric, material, and loading parameters. The bolt–hole contact introduces high localized stress concentrations. Macroscopic observations have revealed that these compressive stresses play an important role in the development of brittle failures around holes [16].

In order to simulate the nonlinear compressive response of wood in pinned joints, Chang [6] used cubic spline interpolation of the experimental curve. Patton-Mallory et al. [15] modeled the nonlinear compression and shear stiffness using a trilinear stress–strain relationship. However, these models do not obey the laws of constitutive modeling in continuum media. Furthermore, there is no coupling between the material behavior in each direction. Others attempted to model wood as elasto-plastic everywhere in a connection [5,14]. The

assumption of elasto-plasticity everywhere in the wood member resulted in theoretically ''unrealistic'' plastified regions due to combined compression/tension at the end of the member or combined tension/tension and shear on the hole-boundary, thus effecting the overall stress-state.

In the present paper, an orthotropic plasticity based compressive material model is proposed to predict the post-elastic deformation caused by local wood crushing under the bolt. The model is implemented in a finite element model of one-bolt timber connection and found to yield reasonable agreement with experimental local and global deformation.

2. Constitutive modeling

Because wood is a cellular and porous material, it can undertake permanent deformation under compression. Some uniaxial compressive tests undergoing large deformation have been performed for different species of wood [8,9] and shown that there is an initial phase with an approximately linear elastic response. Then compression in the axial direction shows some strain softening unlike compression perpendicular to grain and

---

* Corresponding author. Tel.: +1-514-398-6677; fax: +1-514-398-7361.
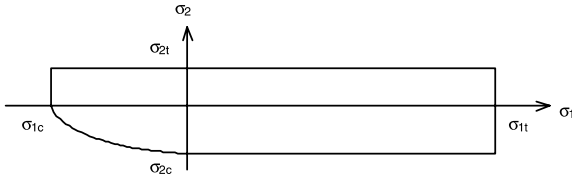*E-mail address:* ghyslaine.mcclure@mcgill.ca (G. McClure).

Fig. 1. Failure envelope of wood (1 = parallel to grain, 2 = perpendicular to grain).

shear. This nonlinear permanent behavior may be described macroscopically within the framework of plasticity theory. Accordingly, wood is modeled as elasto-plastic orthotropic in bi-axial compression according to the Hill yield criterion, and linear elastic orthotropic in tension with the maximum stresses taken as the failure criteria (Fig. 1). Different strength values are considered for tension and compression along each material axis.

2.1. Linear elastic orthotropic constitutive behavior

Although wood microstructure is very complex, it is assumed to be homogeneous. Natural imperfections such as knots, taper, and distortions in the alignment of grain are ignored. If a sample is cut far enough from the centre of the tree so that curvature of the growth rings can be ignored, its properties may then be regarded as orthotropic. It has three orthogonal planes of material symmetry: longitudinal (L), radial (R), and tangential (T). The linear elastic orthotropic constitutive equations can be written in matrix form [4]:

$$\begin{Bmatrix} \varepsilon_{LL} \\ \varepsilon_{TT} \\ \varepsilon_{RR} \\ \gamma_{TR} \\ \gamma_{RL} \\ \gamma_{LT} \end{Bmatrix} = \begin{bmatrix} \frac{1}{E_L} & \frac{-v_{TL}}{E_T} & \frac{-v_{RL}}{E_R} & 0 & 0 & 0 \\ \frac{-v_{LT}}{E_L} & \frac{1}{E_T} & \frac{-v_{RT}}{E_R} & 0 & 0 & 0 \\ \frac{-v_{LR}}{E_L} & \frac{-v_{TR}}{E_T} & \frac{1}{E_R} & 0 & 0 & 0 \\ 0 & 0 & 0 & \frac{1}{G_{TR}} & 0 & 0 \\ 0 & 0 & 0 & 0 & \frac{1}{G_{RL}} & 0 \\ 0 & 0 & 0 & 0 & 0 & \frac{1}{G_{LT}} \end{bmatrix} \begin{Bmatrix} \sigma_L \\ \sigma_T \\ \sigma_R \\ \tau_{TR} \\ \tau_{RL} \\ \tau_{LT} \end{Bmatrix}$$

(1)

where E_L, E_T, E_R are the Young's moduli in directions L, T, R; G_{LT}, G_{TR}, G_{RL} are the shear moduli for planes L–T, T–R, R–L; and v_{ij} is the Poisson's ratio (i, j = L, T, R).

This assumption will be expanded to transverse isotropy, which assumes identical properties in the radial and tangential directions. This combined direction is referred to as perpendicular to grain ($\perp$) while the longitudinal is referred to as parallel to grain ($\parallel$). The constitutive equations are reduced to:

$$\begin{Bmatrix} \varepsilon_1 \\ \varepsilon_2 \\ \gamma \end{Bmatrix} = \begin{bmatrix} \frac{1}{E_1} & \frac{-v_{21}}{E_2} & 0 \\ \frac{-v_{12}}{E_1} & \frac{1}{E_2} & 0 \\ 0 & 0 & \frac{1}{G_{12}} \end{bmatrix} \begin{Bmatrix} \sigma_1 \\ \sigma_2 \\ \tau \end{Bmatrix}$$

(2)

where E_1, E_2 are the Young's moduli in directions $\parallel$ and $\perp$ to grain, respectively; G_{12} is the shear modulus for plane 1–2; and v_{12} is the Poisson's ratio.

It is presumed that $v_{12}E_2 = v_{21}E_1$ [4]. All parameters are determined experimentally.

2.2. Elasto-plastic orthotropic constitutive behavior

2.2.1. Historical background

The incremental plasticity is a macroscopic constitutive model that accounts for dissipative (irreversible) effects characterized by permanent strain accumulation. Hill was the first to conduct studies on anisotropic plasticity [11]. He postulated the form of the yield surface as an extension to von Mises criterion for isotropic materials. Only isotropic hardening was considered leading to a proportional change of the orthotropic parameters during hardening. His work was later extended to account for nonproportional hardening [20], differences in strengths for tension and compression [17], other updated yield surfaces [10] and softening behavior [13]. Implementation of anisotropic plasticity in finite element modeling was achieved in 2-D and 3-D to analyze the behavior of multilayered composite laminates. The model is being incorporated in some finite element softwares with differing assumptions. However, they do not allow the user to define different yield or failure surfaces in tension and compression.

2.2.2. Theory and application to wood

A theory of plasticity is a procedure by which a set of constitutive equations for a multiaxial stress state can be derived from uniaxial stress–strain test data. This is accomplished based on three basic properties: a yield criterion, a flow rule, and a hardening rule [7]. In what follows, the general analytical formulation of the foregoing items will be presented with the application to wood in compression.

2.2.2.1. *Yield criterion.* A generalization of the yield condition for plastically anisotropic materials is the general quadratic function f given by Shih and Lee [17]:

$$f = (\sigma_{ij}, \alpha_{ij}, A_{ijkl}, k) = 0 \tag{3}$$

where σ_{ij} is the second order stress tensor, A_{ijkl} ($i, j, k, l = 1, 2, 3$) denotes the fourth order tensor of anisotropic strength parameters describing the shape of the yield surface, α_{ij} describes the origin of the yield surface and k is a scalar parameter which stands for a reference yield stress.

In particular, a yield function that can capture orthotropy in the strength properties has been proposed by Hill [11] as an extension of the von Mises criterion for isotropic materials. As was demonstrated by François [8], the limit state in compression for some species of wood can be approximated using this criterion. In plane

stress and assuming transversely isotropic medium, the criterion for bi-axial compression can be expressed as:

$$f = \left(\frac{\sigma_1}{\sigma_{1c}}\right)^2 + \left(\frac{\sigma_2}{\sigma_{2c}}\right)^2 + \left(\frac{\tau}{S}\right)^2 - \frac{\sigma_1 \sigma_2}{\sigma_{1c}^2} - 1 = 0 \qquad (4)$$

where σ_1 is the compressive stress $\parallel$ to grain; σ_{1c} is the compressive strength $\parallel$ to grain; σ_2 is the compressive stress $\perp$ to grain; σ_{2c} is the compressive strength $\perp$ to grain; τ is the shear stress; and S is the shear strength.

σ_{1c}, σ_{2c}, and S are material properties and determined experimentally.

f can alternatively be expressed in terms of the effective stress σ_e as follows if hardening is to be modeled:

$$f = \sigma_e - k(\chi) = 0 \qquad (5)$$

where,

$$\sigma_e = (A_{ij}\sigma_i\sigma_j)^{1/2} \qquad (6)$$

and χ termed hardening parameter, and can be related to some measure of plastic deformation or plastic work.

A_{ij} is defined as:

$$A_{ij} = k^2 \begin{bmatrix} \frac{1}{\sigma_{1c}^2} & \frac{-1}{2\sigma_{1c}^2} & 0 \\ \frac{-1}{2\sigma_{1c}^2} & \frac{1}{\sigma_{1c}^2} & 0 \\ 0 & 0 & \frac{1}{S^2} \end{bmatrix} \qquad (7)$$

2.2.2.2. Decomposition of the total strain increments. In the theory of plasticity, it is assumed that the total strain increment, $\{d\varepsilon\}$, consists of plastic components, $\{d\varepsilon^p\}$, and elastic components, $\{d\varepsilon^e\}$

$$\{d\varepsilon\} = \{d\varepsilon^p\} + \{d\varepsilon^e\} = \{d\varepsilon^p\} + [D^e]\{d\sigma\} \qquad (8)$$

$[D^e]$ being the elastic compliance matrix, and can be expressed in terms of the material constants as:

$$[D^e] = \begin{bmatrix} \frac{1}{E_1} & \frac{-v_{21}}{E_2} & 0 \\ \frac{-v_{12}}{E_1} & \frac{1}{E_2} & 0 \\ 0 & 0 & \frac{1}{G_{12}} \end{bmatrix} \qquad (9)$$

2.2.2.3. Flow rule. The flow rule determines the direction of plastic straining and is given as:

$$d\varepsilon^p = d\lambda \frac{\partial f}{\partial \sigma} = d\lambda a \qquad (10)$$

$d\lambda$ being a plastic multiplier that determines the amount of plastic straining, $\partial f/\partial \sigma = a$ is termed the flow vector.

2.2.2.4. Hardening rule. An anisotropic hardening rule developed by Vaziri et al. [19] will be adopted here. Such a theory allows for nonproportional change of the yield values and thus leads to a nonuniform expansion of the yield surface during plastic flow. Based on the notion of equivalent plastic work, the evolution of yield stresses is

assumed to be governed by the following set of equations:

$$\sigma_{1c}^2 - \sigma_{1c0}^2 = \frac{E_{p1}}{H}(k^2 - k_0^2)$$

$$\sigma_{2c}^2 - \sigma_{2c0}^2 = \frac{E_{p2}}{H}(k^2 - k_0^2) \qquad (11)$$

$$\tau^2 - \tau_0^2 = \frac{G}{H}(k^2 - k_0^2)$$

k_0 and k are the initial and updated effective yield stresses, respectively.

E_{p1}, E_{p2}, G_p are the plastic moduli defined by:

$$E_{p1} = \frac{E_1 E_{T1}}{E_1 - E_{T1}}$$

$$E_{p2} = \frac{E_2 E_{T2}}{E_2 - E_{T2}} \qquad (12)$$

$$G_p = \frac{G G_T}{G - G_T}$$

with E_{T1}, E_{T2}, and G_T being the tangent moduli of the stress–strain curves.

H is the plastic modulus of the effective stress–effective strain diagram which can be identified with any one of the three basic stress–strain curves.

$$H = \frac{d\sigma_\varepsilon}{d\varepsilon_\varepsilon} \qquad (13)$$

As mentioned earlier, wood undergoes softening in compression parallel to grain and hardening perpendicular to grain. Depending on the chosen value of H, perfect plasticity, slight hardening or softening can be modeled.

2.2.2.5. Incremental elasto-plastic constitutive equations. The consistency condition requires the state of stress to remain on the yield or loading surface during plastic flow and is expressed by:

$$df = 0 \qquad (14)$$

By substituting Eq. (4) in (14) and combining Eqs. (8) and (10), the constitutive equations are given by [2]

$$d\sigma_{ij} = C_{ij}^{ep} d\varepsilon_j \qquad (15)$$

$$C_{ij}^{ep} = C_{ij}^e - \frac{C_{ik}^e a_k a_l C_{lj}^e}{\left(1 - \frac{1}{2k}\sigma_i\sigma_j\frac{\partial A_{ij}}{\partial k}\right)H' + a_m C_{mn}^e a_n} \qquad (16)$$

C^e is the elastic stiffness matrix, and C^{ep} is termed the elasto-plastic stiffness matrix.

3. Finite element implementation

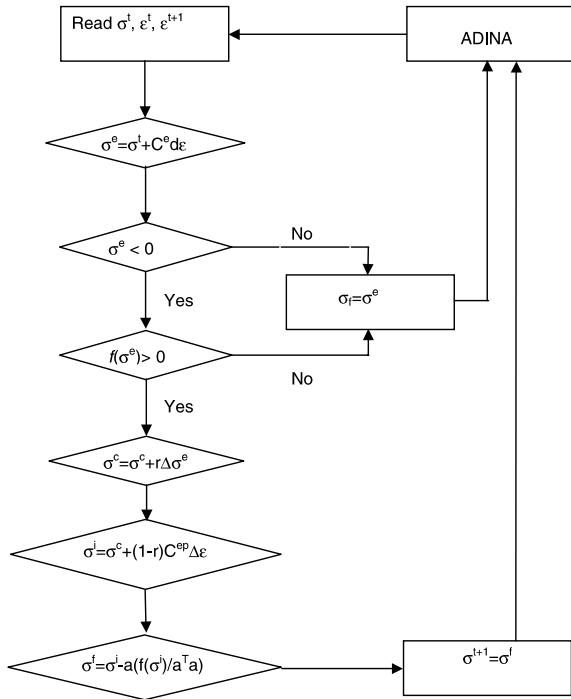A Fortran program of the elasto-plastic compressive material model was written and inserted into the

Fig. 2. Stress computation in the elasto-plastic regime.

user-supplied material model of ADINA software [1]. The flowchart shown in Fig. 2 summarizes the stress computation in the elasto-plastic regime.

4. Application to one-bolt connection

A one-bolt connection model is developed using ADINA and results are compared with new experiments conducted on one-bolted timber connections. The wood member is 17 mm thick loaded by a bolt with a 1 mm radial clearance (Fig. 3). Strains are measured using strain gages in the contact region 5 mm away from the hole. LVDT's are mounted to record the movement of the wood member relative to the bolt.

A typical finite element mesh is shown in Fig. 4. The material properties are given in Table 1. Frictional contact between the bolt and the hole was modeled using Lagrange multiplier algorithm [3] with a coefficient of friction of 0.7 [18]. The finite element program is run first with the elastic orthotropic material model everywhere in the wood member, then with the application of the new elasto-plastic orthotropic model in order to show the benefits of the proposed model over the elastic material model [12].

Fig. 5 shows a comparison of numerically predicted longitudinal compressive strains in the region of contact
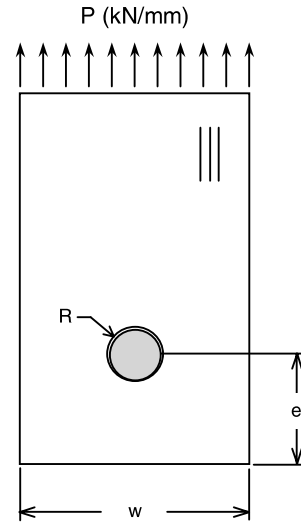

Fig. 3. Schematic of a one-bolt timber connection geometry.
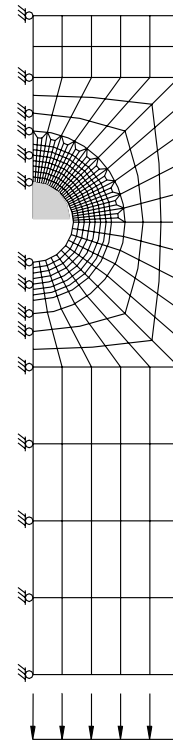

Fig. 4. Finite element mesh of a one-bolt connection.

(a region of high bi-axial compression) with seven replicates of strain gage readings for W1E3 (where w = 1d, e = 3d) and W1E5 (where w = 1d, e = 5d) configura-

Table 1
Material properties for glued-laminated timber

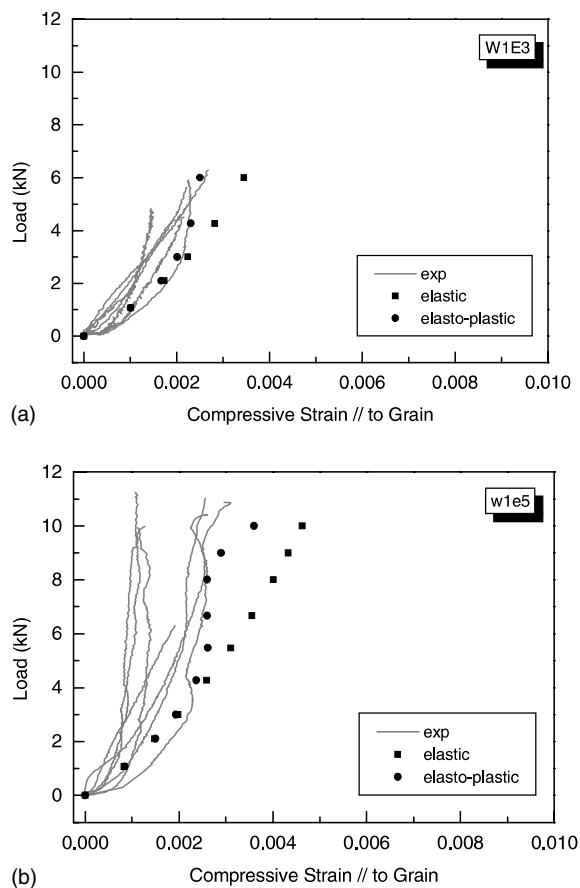| Material property (MPa)	
E_{1c}	9158.8
σ_{1c}	43.8
E_{2c}	325
σ_{2c}	7.70
E_{T1}	14,335
σ_{T1}	102.50
E_{T2}	538
σ_{T2}	6.20
G	756
S	9.10

Fig. 5. Comparison between numerical and experimental compressive strains for (a) W1E3 and (b) W1E5.

tions respectively. The nonlinear behavior of strains observed for both configurations is initially caused by the increased contact between the bolt and the hole. The predicted strains with the linear elastic material model fall in the lower range of the recorded curves and become softer as the load is increased. Better predictions are obtained with the elasto-plastic material model that seems to capture the stiffening behavior of the strains. This becomes more evident in the configuration with longer end distance, i.e. W1E5. At a load approaching the experimental average failure load of about 9 kN, the numerical strains soften since the nodal point enters the plastic state.

To gain further insight into the extent of compression in the contact zone, numerical stresses on the hole-boundary are plotted in Fig. 6 for this group of configurations at their respective average experimental failure loads (5.33 kN for W1E3, and 9.3 kN for W1E5). Compressive stresses parallel and perpendicular to grain substantially exceed the associated strengths with the linear elastic material model (average compressive strengths being $\sigma_\parallel = 43$ MPa and $\sigma_\perp = 8$ MPa), as opposed to the post-elastic material model that increases the contact angle by 30% for W1E3 and 68% for the W1E5 configuration. This angle is found by noting the value on the curves at which the state of stress changes from compression to tension in both directions for each configuration considered.

Numerically predicted load–deformation curves with both material models are compared to those obtained experimentally via LVDT's as shown on Fig. 7 for W1E5 configuration. By modeling wood as elasto-plastic orthotropic, the curve becomes nonlinear, thus agreeing with the experimental trend. This is a major improvement over the linear elastic orthotropic material usually assumed in the modeling of bolted connections. Bearing of the material immediately adjacent to the contact points is causing nonlinear global deformation of the connection.

The spreading of plastic zones and contours of the nondimensional effective stress σ_e/k for the configuration W2E5 are depicted in Fig. 8 for three different load levels: 4, 7, and 10 kN respectively. Incipience of plastic deformation was found to occur right beneath the bolt at a low load of approximately 2 kN. As the loading increases, the plastic zone extends in depth towards the end member in the direction of loading and in large along the hole-boundary. The characteristic shape and growth of the plastic zone at the maximum load, about 10 kN, can be associated with the compressed "column" of material which fails in bearing parallel to grain.

Stress contour plots with both material models further prove the adequacy of the proposed material model to predict the post-elastic behavior of single-bolted connections. Again, these contours are generated at the average experimental failure load for W2E5 configuration (Fig. 9a and b). The contact compression zone is found to increase significantly causing a higher tension zone perpendicular to grain right after the end of contact between the bolt and the hole. This is also causing the region of high shear to shift on the hole-boundary. Net tension caused by high tensile stresses parallel to grain
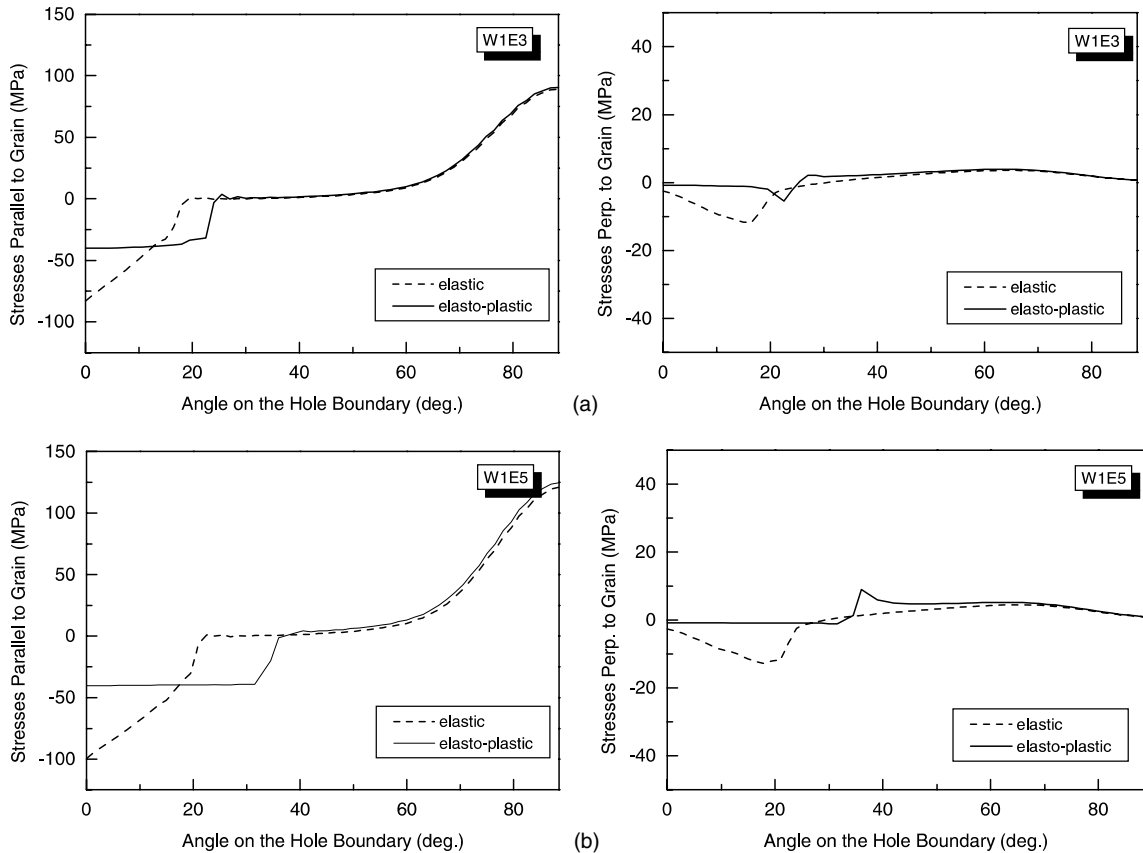
Fig. 6. Predicted stress distribution along the hole-boundary parallel and perpendicular to grain for (a) W1E3 and (b) W1E5.
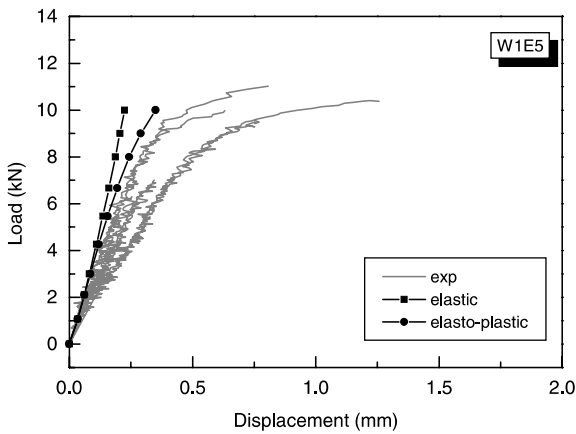

Fig. 7. Comparison between numerical and experimental load vs. deformation curves for W1E5.

and adjacent to the hole is one possible failure mode. Shear-out due to combined shear and tensile stresses perpendicular to grain on the boundary after the contact zone is another possible failure mode. In fact these are the predominant failure modes noted in the experiments.

5. Conclusion

The proposed compressive constitutive material model has improved the predictions of local and global behavior of connections in timber, and given insight into the brittle failure mechanism. It is found that inelastic deformation starts at low load levels beneath the bolt. Bearing of the material immediately adjacent to the contact points is causing nonlinear global deformation of the connection. As loading progresses, a larger contact area between the wood and the bolt is developed, as compared with the linear elastic material model. Failure is believed to be caused by combined effect of shear and tension perpendicular to grain along failure planes that lie either side of the compressed contact zone, thus corresponding to the predominant shear-out failure observed in the experiments.
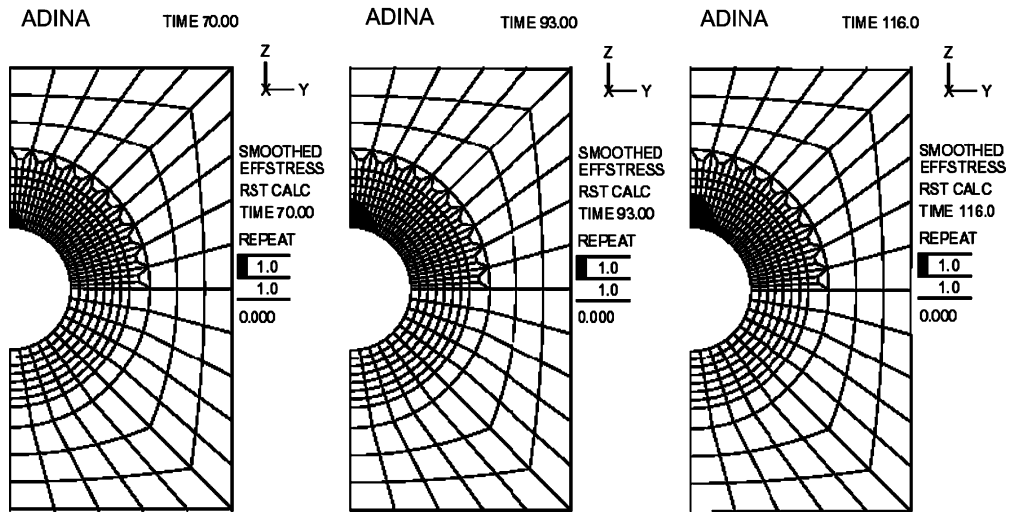
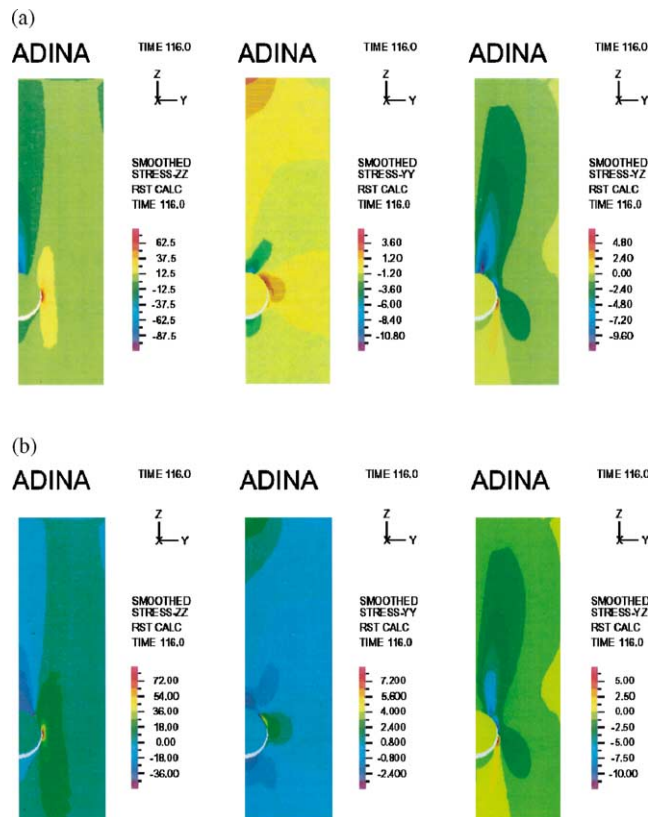Fig. 8. Spread of plasticity in a one-bolt connection W2E5.

Fig. 9. (a) Elastic stress distribution in a one-bolt connection W2E5. (b) Elasto-plastic stress distribution in a one-bolt connection W2E5.

Acknowledgements

References

[1] ADINA R&D Inc. Theory and modeling guide, Report ARS 95-8, Watertown, MA, 1995.

[2] Bathe KJ. Finite element procedures. Englewood Cliffs, New Jersey: Prentice-Hall; 1996.

[3] Bathe KJ, Chaudhary A. A solution method for planar and axisymmetric contact problems. Int J Numer Meth Eng 1985;21:65–88.

[4] Bodig J, Jayne BA. Mechanics of wood and wood composites. New York: Van Nostrand Reinhold; 1982.

[5] Bouchair A, Vergne A. An application of the Tsai criterion as a plastic flow law for timber bolted joint modelling. Wood Sci Technol 1995;30:3–19.

[6] Chang YJ. Design of mechanical joints in composites. PhD thesis, Department of Mechanical Engineering, University of Wisconsin, Madison, 1983.

[7] Chen WF, Han DJ. Plasticity for structural engineers. New York: Springer Verlag; 1988.

[8] François P. Plasticité du Bois en compression multiaxiale, application à l'absorption d'énergie mécanique. Thèse de Docteur de l'université Bordeaux, Bordeaux I, France, 1992.

[9] Gibson LJ, Ashby MF. Cellular solids—structure and properties. Oxford, New York: Pergamon Press; 1988.

[10] Gotoh M. A theory of plastic anisotropy based on a yield function of fourth order (plane stress state). Int J Mech Sci 1978;19:505–20.

[11] Hill R. The mathematical theory of plasticity. Oxford, NY: Oxford University Press; 1950.

[12] Kharouf N. Post-elastic behavior of bolted connections in wood. PhD thesis, Department of Civil Engineering and Applied Mechanics, McGill University, Montreal, Canada, 2001.

[13] Lourenço B, De Borst R, Rots JG. A plane stress softening plasticity model for orthotropic materials. Int J Numer Meth Eng 1997;40:4033–57.

[14] Moses MD, Prion HGL. Bolted connections in structural composite lumber: anisotropic plasticity approach. In: Walford GB, Gaunt DJ, editors. Proceedings of Pacific Timber Engineering Conference, Rotorua, New Zealand, 14–18 March, 1999, p. 92–9.

[15] Patton-Mallory M, Pellicane PJ, Smith IW. Nonlinear material models for analysis of bolted wood connections. ASCE J Struct Eng 1997;123(8):1063–70.

[16] Rodd PD. The analysis of timber joints made with circular dowel connectors. PhD thesis, University of Sussex, Brighton, UK, 1973.

[17] Shih CF, Lee D. Further developments in anisotropic plasticity. Trans ASME, J Eng Math Technol 1978; 100:294–302.

[18] Smith I. Coefficient of friction values applicable to contact surfaces between mild steel connectors such as bolts and dry European white wood. J Inst Wood Sci 1983:229–34.

[19] Vaziri R, Olsen MD, Anderson DL. Finite element analysis of fibrous composite structures: a plasticity approach. Comput Struct 1992;44:103–16.

[20] Whang B. Elasto-plastic plates and shells. In: Proceedings of the Symposium on Application of Finite Element Method in Civil Engineering, Vanderbilt University Tennessee, 1969, p. 481–515.